Journal of CO_2 Utilization 22 (2017) 289–298

Contents lists available at ScienceDirect

Journal of CO_2 Utilization

journal homepage: www.elsevier.com/locate/jcou

Transient analysis of the reverse water gas shift reaction on Cu/ZrO_2 and $Ga_2O_3/Cu/ZrO_2$ catalysts

Esteban L. Fornero, Dante L. Chiavassa, Adrian L. Bonivardi, Miguel A. Baltanás*

INTEC (Instituto de Desarrollo Tecnológico para la Industria Química—UNL/CONICET), Güemes 3450, S3000GLN Santa Fe, Argentina

ARTICLE INFO

Keywords:
CO_2 hydrogenation
Methanol synthesis
Water gas shift
Supported copper
Redox mechanism
Associative mechanisms

ABSTRACT

The performance of two copper-based catalysts, Cu/ZrO_2 and $Ga_2O_3/Cu/ZrO_2$, in regards the reverse water gas shift (RWGS) reaction as compared with their reaction rates for the methanol synthesis reaction (R_{CH3OH}) was studied using H_2/CO_2 mixtures at 1.6 and 0.1 MPa, at 498 K. The reactivity studies were carried out using a Carberry-type microcatalytic reactor operated in the batch (transient) mode after H_2 prereduction at 523 K (2 h).

Measurements of the catalytic activity were also made using D_2/CO_2 mixtures (0.1 MPa, 498 K) to assess isotope effects. For Cu/ZrO_2, the initial RWGS reaction rate using D_2 instead of H_2 was slightly higher whereas such rate was about equal for the ternary catalyst.

Kinetic rate expressions obtained from the Langmuir-Hinshelwood-Hougen-Watson formalism were used to model and analyze the experimental results and the reaction mechanism(s) of the RWGS on these catalysts. Congruence was found between the experimental results and a reaction mechanism where (predominantly) CO_2 adsorbs dissociatively on the Cu particles (rate-determining step). The reduction of (ad)oxygen and surface hydroxyls follow afterwards.

1. Introduction

The water gas shift (WGS) reaction, significantly important in many industrial processes, has been broadly studied on supported metal, copper-based commercial catalysts such a $Cu/ZnO/Al_2O_3$, which are generally used in the low temperature range (470–520 K) [1]. Comparatively, the reverse water gas shift (RWGS) reaction has attracted less attention, in part because it is not industrially used, and is only present whenever hydrogen and carbon dioxide coexist in the reaction mixture. Nowadays, both compounds are used in the synthesis of many products (e.g., CH_3OH, CH_4, dimethyl ether (DME), etc.), and the RWGS is one of the reactions that diminishes the selectivity of such processes. In the methanol synthesis, for example, the two competing reactions are the following:

$$CO_2 + 3\,H_2 \rightleftarrows CH_3OH + H_2O \qquad (R_{CH3OH})$$

$$CO_2 + H_2 \rightleftarrows CO + H_2O \qquad (R_{RWGS})$$

Therefore, it is crucial to fully understand the mechanism(s) through which the RWGS proceeds, so as to be able to control it, and improve selectivity.

In general, two different mechanisms for the direct and/or the reverse water gas shift reactions have been postulated: dissociative and associative [2]. In the first one, also named regenerative or redox, the reactants are oxidized or reduced separately on the catalyst surface:

$$H_2O + {}^\circ \rightleftarrows H_2 + O - {}^\circ$$

$$O - {}^\circ + CO \rightleftarrows CO_2 + {}^\circ,$$

whereas in the associative mechanism the reaction occurs via a surface intermediate:

$$CO + H_2O \rightleftarrows \text{intermediate}$$

$$\text{intermediate} \rightleftarrows CO_2 + H_2$$

The nature and the reaction mechanism of the RWGS using copper-based catalysts (not only commercial materials, but also Cu/SiO_2 and/or Cu single crystals) are still under debate. The dissociative mechanism has been generally postulated [1,3–7], although, depending on pressure, temperature and composition of the feed, it has also been reported that CO may be produced on copper via an associative mechanism [4,7–14]. With regard to the latter one, formate has been traditionally postulated as the key intermediate [13–15]. More recently, however, some DFT studies have suggested that carboxyl is the key intermediate in the associative mechanism of the RWGS reaction on copper

* Corresponding author.
E-mail address: tderliq@santafe-conicet.gov.ar (M.A. Baltanás).

http://dx.doi.org/10.1016/j.jcou.2017.06.002
Received 30 March 2017; Received in revised form 25 April 2017; Accepted 2 June 2017

[7,9–11,16] and that formate is just a surface spectator [7,9]. Yet, the likelihood of both mechanisms proceeding simultaneously has also been put forward as well [16,17].

Concerning Cu/ZrO_2 catalysts, Fisher and Bell [12] postulated that the RWGS occurs mostly on the metal because, upon comparing Cu/silica catalysts with and without added ZrO_2, the rate of said reaction was not significantly enhanced. Meanwhile, Wokaun and coworkers postulated that CO_2 and CO can interconvert −on the support- via a formate intermediate, endorsing an associative, bifunctional mechanism [13,14].

For methanol synthesis, and using H_2/CO_2/He mixtures, ternary catalysts based on Cu-Ga-Zr presented similar yield, but higher selectivity to the alcohol, in comparison with their binary Cu-Zr counterparts [18]. Said behavior was observed both under steady state and under *initial,* transient conditions (that is, evaluating only the synthesis of the alcohol together with the RWGS from CO_2 with independence of the dry methanol synthesis from CO and/or the alcohol decomposition [19]). This last type of experiments showed that the intrinsic selectivity of the ternary catalyst was superior.

At first sight, then, the RWGS activity of both catalysts appeared as substantially different. So, we judged interesting to progress in the study of these materials (which belong in the class of "sinergetic catalysts" [7], alternative to the conventional, commercial methanol synthesis catalysts), to increase the understanding − and eventually unravel the underlying causes − of such observations and identify more explicitly the roles of each component of the catalysts in the reaction.

Our ultimate goal is, then, to identify the main reaction pathway(s) of the RWGS in Cu-Zr and Cu-Ga-Zr catalysts and estimate quantitatively the likelihood of the existence of more than just one mechanism acting simultaneously. For this purpose, the catalytic activity for the RWGS reaction was evaluated under differential conversion conditions at intermediate and low (atmospheric) pressure, seeking thus to disengage its analysis from the remaining reactions that occur in the methanol synthesis. Besides, the existence (or lack) of kinetic isotope effect in the RWGS was studied by substituting hydrogen for deuterium, and the initial reaction rate expressions resulting from the proposed competing mechanisms were compared so as to discriminate between the different kinetic models.

We believe that this (chemical reaction engineering-based modeling) approach may provide substantial, new elements for the rational design of novel catalysts, like Cu-Ga-Zr, capable of overcoming present hurdles, such as process selectivity, in the synthesis of methanol from CO_2.

2. Experimental

2.1. Catalysts preparation

Two Cu/ZrO_2 and $Ga_2O_3/Cu/ZrO_2$ catalysts were prepared as already detailed in previous work [18,19]. Briefly, zirconia was synthesized via the sol-gel method. After drying and calcining in air (383 and 673 K, resp.), the specific surface area of the pure ZrO_2 was 35 m^2/g (determined by the Brunauer-Emmett-Teller method). Copper was incorporated by ion exchanging an aqueous solution of ammonia copper complexes at pH 11 (mainly $[Cu(NH_3)_4]^{2+}$) with the powdered support, for 2 h, under stirring. The liquid volume to solid mass ratio was 200 ml/g. Next, the suspension was filtered and washed for 15 min with NH_4OH(aq), at pH 11. This procedure was repeated twice. The material was then dried and air calcined (383 and 673 K, resp.). The metal loading of the binary Cu/ZrO_2 catalyst so obtained was 2.6 wt.% and the specific surface area was 29 m^2/g. After reducing at 553 K the metal dispersion, measured by reactive frontal chromatography [20], was 5.4%.

Gallium oxide was incorporated to an aliquot of the calcined Cu/ZrO_2 catalyst by incipient wetness impregnation of $Ga(NO_3)_3$ in aqueous solution (3.8 wt.% of Ga_2O_3; Ga/Cu = 1/1 at./at.). The dried and calcined (673 K) $Ga_2O_3/Cu/ZrO_2$ catalyst had a specific surface area of 9 m^2/g and, after reduction at 553 K, the metal dispersion was then 2%. No incorporation of Cu^{2+} or Ga^{3+} ions into the structural network of the zirconia, nor any peak of segregated crystallized Ga_2O_3 phase(s), were observed by XRD, thus suggesting only the presence of highly dispersed, amorphous gallia [18]. A detailed characterization of these ternary Cu-Ga-Zr catalysts by TPR and XPS, where the copper-gallia interaction was purposely analyzed, can be found elsewhere [21].

2.2. Catalytic activity measurements

All reactivity studies were carried out using a Carberry-type microcatalytic reactor operated in the batch (transient) mode, whose manufacture and operational features were presented recently by some of us [22]. Briefly, the reactor consists of a small, removable, magnetically stirred spinning basket that can be filled with the crushed and sieved catalyst, located inside a leak valve (volume: ~ 37 cm^3). The valve allows the continuous sampling of the gas content to a mass spectrometer at the expense of only a small pressure change inside the microreactor. The complete set up features a premixer of the reaction mixture and a high rating bellows valve to fill the microreactor from the premixer. All the internal parts were gold-plated to ensure inertness.

Cylindrical tablets of 1 cm diameter and approx. 0.25 mm thickness of both catalysts, as well as the support, were prepared using a laboratory press. The tablets were crushed and sieved (−20/+30 Tyler mesh, 0.5–0.8 mm) prior to placing the solid particles inside the reactor baskets.

For every experimental run a fresh batch of each material was loaded into the reactor and reduced *in situ* in flowing H_2 (50 ml/min), using a heating ramp of 2 K/min, from room temperature to 523 K (i.e., enough to ensure copper reduction) [21], and then keeping this last temperature for 2 h. Next, still under H_2 flow, the reactor was cooled down to the selected reaction temperature (498 K) and evacuated (600 Pa) for 20 min prior to catalytic evaluation. Given the geometric dimensions of the particles used, and the magnitude of initial reaction rates that were measured, the reaction system always operated within the kinetic regime [22]. Blank runs using just the empty microreactor and/or loading it with the ZrO_2 support were performed. In either case, no reactants conversion was observed.

A 64-channel mass spectrometer (Residual gas analyzer Balzers QMS 421, 0–300 amu range), with a QMH 400-5 quadrupole and SEM and Faraday cup detectors was employed to measure continuously the gas composition inside the microreactor. Two daily calibrations were performed to correlate the signal intensities in the MS with the respective molar fraction of each component inside the microreactor, for the full range of expected concentrations. The first calibration was made using a blank run. To calibrate the signals of the reaction products, a gas mixture with the thermodynamic equilibrium composition at same temperature and pressure was used instead. More details about these MS measurements can be found in a previous work [22].

Ultra high purity gases were used (H_2, He and Ar INDURA, grade 5; H_2/CO_2/He = 75/22/3 v/v, INDURA certified mixture; CO_2 and CO, 99.99% pure). Silicagel was used to eliminate water traces in both, H_2 and the H_2/CO_2/He gas mixtures. CO was purified using crushed quartz (-20/+30 Tyler mesh) at 473 K, to decompose metal carbonyls. The deuterium used was Scott CP grade, 99.7%, with no further purification.

2.2.1. Medium pressure measurements (Methanol synthesis activity)

The catalytic performance of Cu/ZrO_2 and $Ga_2O_3/Cu/ZrO_2$ (approx. 1 g/ea.) was first evaluated at 1.6 MPa and 498 K, using a H_2/CO_2/He = 75/22/3 v/v mixture. After 2 h the reactor was evacuated (600 Pa) for 20 min. The gas mixture was again introduced into the reactor under the same reaction conditions (1.6 MPa and 498 K) and

kept for 40 min. The evacuation/reaction procedure was repeated once more. In what follows the three sequential reaction events will be designated as runs 'am', 'bm' and 'cm'. Two calibration mixtures were used to take these measurements, with $H_2/CO_2/He$ = 75/22/3 v/v and $H_2/CO_2/CO/CH_3OH/H_2O/He$ = 70/19/2.4/1.6/4/3 v/v.

2.2.2. Atmospheric pressure measurements (Reverse water gas shift activity)

Approximately 0.1 g of each material was used to evaluate their catalytic performance at 0.1 MPa and 498 K, using a $H_2/CO_2/Ar$ = 66/22/12 v/v mixture prepared in the premixer. After 40 min the reactor was evacuated (600 Pa) for 20 min. The gas mixture was again introduced under the same reaction conditions (0.1 MPa and 498 K) and kept for 40 min. The evacuation/reaction procedure was repeated once more. From now on, the three sequential reaction events will be designated as runs 'al', 'bl' and 'cl'. Two calibration mixtures were used to take these measurements, with $H_2/CO_2/Ar$ = 66/22/12 v/v and $H_2/CO_2/CO/H_2O/Ar$ = 63/19/3/3/12 v/v.

To assess in more detail the superficial change(s) of the Cu/ZrO_2 catalyst between the initial reduced state to the 'operational state' in the synthesis and the RWGS reactions, its performance was also evaluated at 0.1 MPa and 498 K with a $H_2/CO_2/Ar$ = 30/30/40 v/v gas mixture, using 1 g of catalyst and the same experimental protocol described before for the 'al' run. After 40 min of reaction the microreactor was evacuated (600 Pa) during 20 min and then a H_2/Ar = 30/70 v/v mixture was introduced (0.1 MPa), to analyze the reactivity toward hydrogen of the species chemisorbed onto the catalyst surface.

The performance of each catalyst was also evaluated using a $D_2/CO_2/Ar$ = 66/22/12 v/v mixture (approx. 0.1 g/ea., at 0.1 MPa and 498 K), to appraise the impact of any isotope effect in the RWGS. The experimental procedure was similar to that described in the previous paragraphs with just slight modifications, namely: prior to the first dose of the reaction mixture the materials were reduced with pure D_2 (50 ml/min, 30 min) at 498 K, so as to replace all of the surface hydrogen species left by the initial reduction with H_2 for 2 h. Only two consecutive runs ('alD' and 'blD') were made in this case. The calibration mixtures used to take these last measurements were $D_2/CO_2/Ar$ = 66/22/12 v/v and $D_2/CO_2/CO/D_2O/Ar$ = 63/19/3/3/12 v/v.

3. Results and discussion

3.1. Catalytic performance at medium pressure

Fig. 1 shows the results obtained for Cu/ZrO_2 at 1.6 MPa ($H_2/CO_2/He$ = 75/22/3 v/v, 498 K) during the first experimental run, made right after the reduction of the catalyst (run 'am'). The Supplementary material section contains the results corresponding to the consecutive runs performed with the catalyst, 'bm' and 'cm' (Figs. S.1 and S.2), as well as the ones for the complete set of experimental runs done with $Ga_2O_3/Cu/ZrO_2$ (Figs. S.3–S.5). The equilibrium composition of the reacting system (indicated with straight lines, for each component) calculated by considering the initial pressure inside the reactor and a pressure drop of 0.1 MPa/h due to the continuous gas sampling from the leak valve, is also given in the figure.

A continuous decrease of the molar fractions of CO_2 and H_2 with reaction time inside the reactor, as well as the increase of those of CH_3OH, CO and H_2O, can be readily appreciated in the figure. Noteworthily, in all these experiments the molar fractions of dimethyl ether and methane were always less than 0.01 and 0.05%, respectively. For the transient reaction period ("onset"), the molar fractions of hydrogen and water could not be measured without significant uncertainty (dashed lines in Fig. 1). This is due to the relatively high background pressure of said components inside the sampling chamber of the mass spectrometer before the start of the transient experiment, as a result of the previous pre-reduction of the catalyst with H_2 [22].

Because the synthesis reaction features a change in the number of moles, $\Delta\nu$, the equilibrium molar fractions in the reacting system are pressure-dependent. Therefore, initial reaction rates were estimated using only the experimental data taken during the first 20 min, where the equilibrium molar fraction of methanol only decreases by approx. 3%.

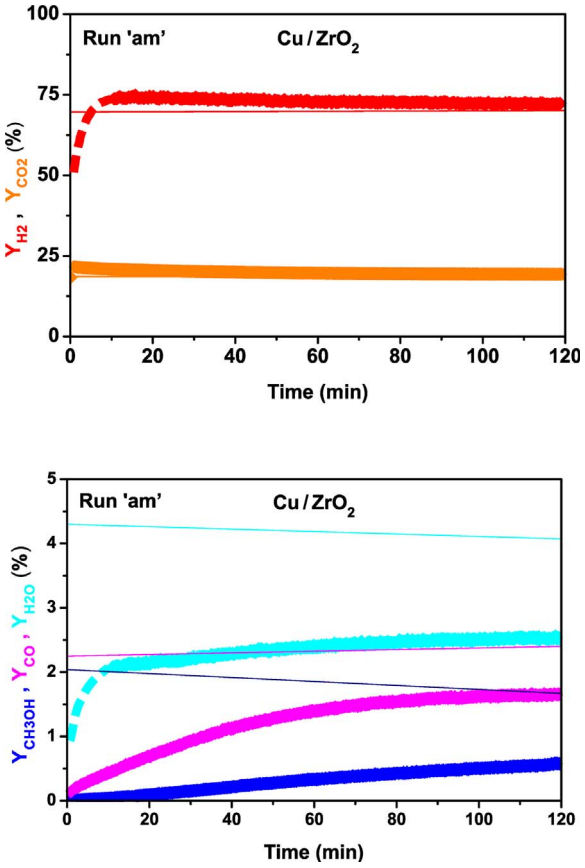

Fig. 1. Methanol synthesis activity at medium pressure on Cu/ZrO_2 (gas mixture: $H_2/CO_2/He$ = 75/22/3 v/v; run 'am') at 1.6 MPa, 498 K (1 g cat.): Y_{H2}, red. Y_{CO2}, orange. Y_{CH3OH}, blue. Y_{CO}, magenta. Y_{H2O}, light blue. Straight lines: Y_{XX}^{eq} (See text). (For interpretation of the references to colour in this figure legend, the reader is referred to the web version of this article.)

An enlargement of Fig. 1 that shows the first minutes of the experimental run 'am' is shown in Fig. 2 (the Supplementary material section contains the enlarged view of this period for all the consecutive runs made with both catalysts, Figs. S.6–S.10). After less than 2 min the increase in the molar fractions of CH_3OH and CO with time was

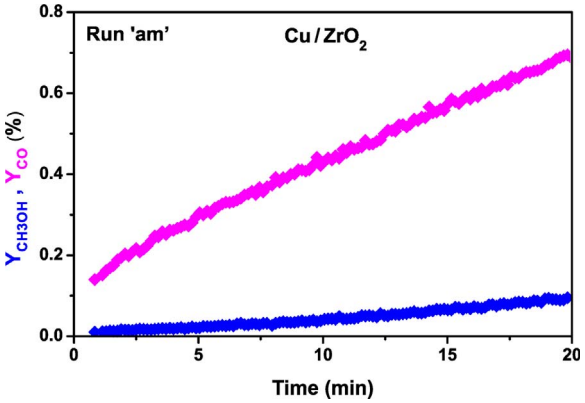

Fig. 2. Initial catalytic activity in the methanol synthesis at medium pressure on Cu/ZrO_2 (gas mixture $H_2/CO_2/He$ = 75/22/3 v/v; run 'am') at 1.6 MPa, 498 K (1 g cat.): Y_{CH3OH}, blue. Y_{CO}, magenta.(For interpretation of the references to colour in this figure legend, the reader is referred to the web version of this article.)

practically linear but, also, there was a "onset concentration shift" in the measured molar fractions for both products during the first minute (which diminished in the consecutive runs, 'bm' and 'cm').

This last behavior is related to changes in the surface composition of the supported metal catalyst from a completely reduced state, in which only the presence of atomic hydrogen and hydroxyls was expected, to an "operating state" where copper is no longer completely reduced, due to the presence of the CO_2 reactant (see below). Additionally, as finely described by Bell [12,23–25] and Wokaun [13,14] research teams, reactive carbonaceous species (which constitute reservoirs of intermediates that ultimately lead to the reaction products observable in the gas phase) built-up onto the support. Said reservoirs of intermediates were generated in the first experimental run (the one labeled as 'am'), carried out with the freshly reduced catalyst while, instead, at the onset of the consecutive runs 'bm' and 'cm' some of these intermediates (which were not completely removed after evacuating down to 600 Pa for 20 min at 498 K) were still present on the catalyst surface.

Taking these observations into account, the *initial* reaction rates of R_{CH3OH} and R_{CO} were calculated using the time period between 3 and 20 min, so as to avoid the inclusion of the transient changes occurring on the catalyst' surface at the reaction onset (0–3 min). The complete set of experimental data of the CH_3OH and CO molar fractions (Y_{CH3OH} and Y_{CO}) comprised within the chosen time interval could be fit with straight lines. Table 1 presents the calculated values of R_{CH3OH} and R_{CO} for Cu/ZrO_2 and $Ga_2O_3/Cu/ZrO_2$ for the three consecutive runs ('am', 'bm' and 'cm'), obtained from the slopes of the almost linear evolution of Y_{CH3OH} and Y_{CO}, together with the percent selectivity to methanol (S_{CH3OH} %) calculated from both initial rates [19]. It is apparent that in all of the consecutive runs the gallium promoted catalyst was more selective to methanol than the binary one, Cu/ZrO_2.

It is worth mentioning that as compared with the first run ('am') the binary catalyst showed a higher reaction rate for the methanol synthesis (and therefore even greater S_{CH3OH}) in the consecutive runs. This apparently anomalous behavior might well be ascribed to the presence of a residual amount of chemisorbed water acting as promoter in the subsequent runs, which was recently also observed by Campbell and coworkers on Cu/silica catalysts using the H_2/CO_2 reacting mixture [9]. Likewise, for $Cu/ZrO_2/SiO_2$ Fisher and Bell reported that methoxide adsorbed onto the zirconia (CH_3O-Zr) was converted into methanol by hydrolysis (hydrolytic pathway) faster than by hydrogenation (reductive pathway) [12,23]. Hence, in the consecutive experiments 'bm' and 'cm' residual, adsorbed water may facilitate the conversion of the methoxide generated in previous reaction steps and, consequently, lead to higher methanol reaction rate.

In regards the ternary catalyst, $Ga_2O_3/Cu/ZrO_2$, the observed changes of reaction rate and/or selectivity among the consecutive runs were within the experimental error and so no further insight was possible.

Table 1 also includes the initial rates of CO production measured with the freshly reduced catalysts ('am' runs) normalized by surface area, as well as the corresponding TOF_{CO} values. It can be appreciated that even though the R_{CO} normalized by mass were higher in the binary catalyst than in the ternary one, said rates were approximately equal after surface area normalization, and the TOFs were about the same as well. Thence, it was not possible to discriminate 'a priori' which is the prevailing mechanism for CO production on both catalysts, and additional effort was needed to extract deeper comprehension on this matter (see below).

3.2. Catalytic performance at atmospheric pressure

Experiments were carried out at atmospheric pressure to understand further the performance of both catalysts in the RWGS reaction, and to address issues related to their selectivity in the synthesis of methanol. The underlying rationale for this approach was that, because the partial order of reaction for hydrogen in the main (methanol synthesis) reaction is smaller than in the RWGS reaction [26–28], the relative rate of the former decreases significantly at lower pressure and, therefore, atmospheric pressure experiments allow focusing on the RWGS reaction instead.

Fig. 3 details the time evolution of the molar fraction of CO, Y_{CO}, for the consecutive experiments made under these new conditions (0.1 MPa, 498 K, $H_2/CO_2/Ar$ = 66/22/12 v/v) with Cu/ZrO_2 and $Ga_2O_3/Cu/ZrO_2$ (runs labeled 'al', 'bl', and 'cl'), respectively. The time evolution of the molar fractions of the remaining components in the reacting system is shown in the Supplementary material section, Figs. S.11-S.16. The only compounds that were detected in these experiments were those of the RWGS proper: H_2, CO_2, CO and H_2O. The measured molar fractions of hydrogen and water were only representative of their true values inside the microreactor after a few minutes, as explained above.

As Fig. 3 shows, for Cu/ZrO_2 there was a pronounced, progressive decrease in CO production during the transient reaction period (onset) throughout the three consecutive runs. This behavior could not be fully perceived, though, with the ternary catalyst, $Ga_2O_3/Cu/ZrO_2$, most likely due to the low values of Y_{CO}, closer to the detection limit of the mass spectrometer.

In addition, during the first run performed with Cu/ZrO_2 (run 'al') the recorded molar fraction of water was consistently lower than that of carbon monoxide (which would imply lack of mass balance closure if only the RWGS reaction was considered, see Fig. S.11). Said feature was

Table 1
Initial values of the reaction rates for methanol (R_{CH3OH}) and carbon monoxide (R_{CO}) production, and percent selectivity to methanol (S_{CH3OH} %) at medium pressure, for Cu/ZrO_2 and $Ga_2O_3/Cu/ZrO_2$. Experimental conditions: $H_2/CO_2/He$ = 75/22/3 v/v; T = 498 K; P = 1.6 MPa; 1 g cat. Consecutive runs: 'am', 'bm' and 'cm' ('*Initial*' stands for experimental data taken after the reaction onset − See text).

Catalyst	$R_{CH3OH} \times 10^8$ (mol/g_{cat}.s)[a,b]			$R_{CO} \times 10^8$ (mol/g_{cat}.s)[c,b]			S_{CH3OH} (%)[f]		
	Run			Run			Run		
	'am'	'bm'	'cm'	'am'	'bm'	'cm'	'am'	'bm'	'cm'
Cu/ZrO_2	1.11	1.94	2.33	6.42 (0.22)[d] (2.91×10^{-3})[e]	6.75 (0.23)[d]	7.70 (0.27)[d]	15	22	23
$Ga_2O_3/Cu/ZrO_2$	1.92	1.49	1.59	2.46 (0.27)[d] (3.07×10^{-3})[e]	2.46 (0.27)[d]	3.04 (0.34)[d]	44	38	34

[a] R_{CH3OH}: $CO_2 + 3H_2 \rightleftarrows CH_3OH + H_2O$.
[b] The values of the coefficient of determination of each linear regression for ΔY_i vs. Δt (i = CH_3OH or CO) within the 3 to 20 min time interval, together with the 95% confidence interval for each estimated rate value is given in Supplementary material, Table S.1.
[c] R_{CO}: $CO_2 + H_2 \rightleftarrows CO + H_2O$ [RWGS].
[d] Parentheses: Surface-normalized rates, $R \times 10^8$ (mol/m^2_{cat}.s).
[e] Turnover frequencies expressed as molecules of CO per copper surface atom per second.
[f] S_{CH3OH} (%) = $R_{CH3OH}/(R_{CH3OH} + R_{CO}) \times 100$.

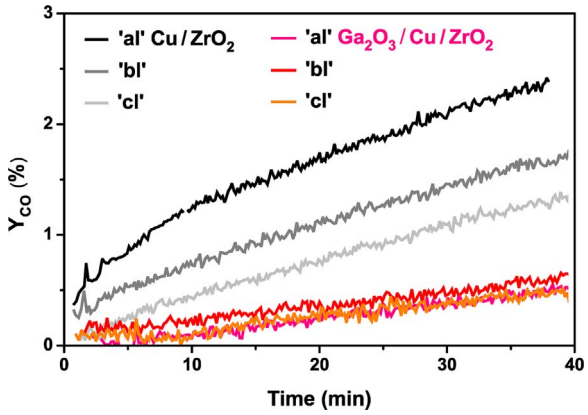

Fig. 3. CO production in the RWGS reaction at atmospheric pressure, for Cu/ZrO_2 and $Ga_2O_3/Cu/ZrO_2$ ($H_2/CO_2/Ar$ = 66/22/12 v/v; runs 'al', 'bl' and 'cl') at 0.1 MPa, 498 K (0.1 g cat.). Y_{CO}^{eq} = 3%.

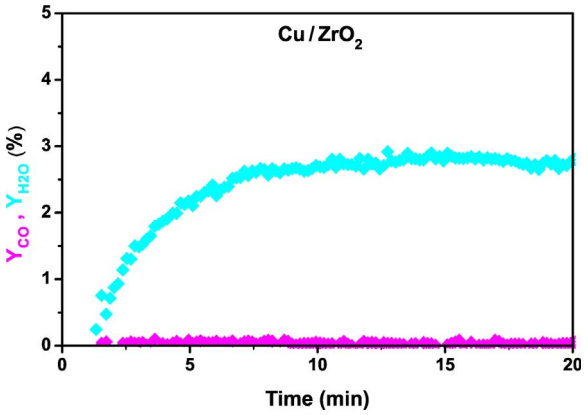

Fig. 5. Post-reaction reduction of Cu/ZrO_2 (gas mixture: H_2/Ar = 30/70 v/v; 1 g cat.) at 0.1 MPa, 498 K: Y_{CO}, magenta. Y_{H2O}, light blue. (For interpretation of the references to colour in this figure legend, the reader is referred to the web version of this article.)

not registered in the following, consecutive runs 'bl' and 'cl' where the mass balance was satisfactory (Figs. S.12 and S.13). These observations are entirely congruent with the occurrence of changes in the surface structure of the supported metal catalyst during the onset (i.e., non-linear) period, from a completely reduced state to one in which atomic and/or molecular (ad)species were formed.

To explore in greater detail these superficial changes in Cu/ZrO_2, which was the material with higher activity for the RWGS reaction, a different gas mixture: $H_2/CO_2/Ar$ = 30/30/40 v/v and a fresh, 10-fold higher mass of catalyst were used (0.1 MPa, 498 K, 1 g cat.). Under these pressure and temperature conditions the equilibrium composition of the gas mixture is: $H_2/CO_2/CO/H_2O/Ar$ = 27.6/27.6/2.37/2.37/40 v/v. As it can be appreciated in Fig. 4 the recorded values of Y_{CO}, at variance with those of Y_{H2O}, were higher than the ones corresponding to chemical equilibrium. This behavior can be explained by recalling the following oxidation reaction (where the • symbol indicates a metal site):

$$CO_2 + \bullet \rightleftarrows CO + O-\bullet \qquad (R_{oxid})$$

In the second stage of this new experiment, vacuum was applied (600 Pa) after 40 min of reaction and only hydrogen was incorporated into the reaction vessel (H_2/Ar = 30/70 v/v, 0.1 MPa and 498 K). Significant production of H_2O, but almost no CO generation was then observed (Fig. 5), which is entirely consistent with the occurrence of the reduction of the previously formed atomic (ad)species:

$$O-\bullet + H_2 \rightleftarrows \bullet + H_2O \qquad (R_{red})$$

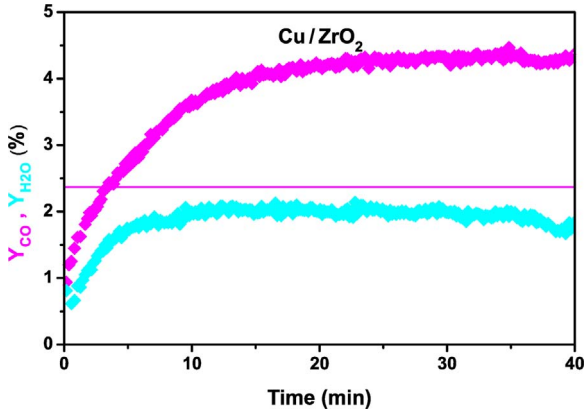

Fig. 4. Catalytic activity in the RWGS reaction on Cu/ZrO_2 (gas mixture H_2/CO_2/Ar = 30/30/40 v/v; 1 g cat.) at 0.1 MPa, 498 K: Y_{CO}, magenta. Y_{H2O}, light blue. Straight line: Y_{XX}^{eq} (See text). (For interpretation of the references to colour in this figure legend, the reader is referred to the web version of this article.)

The traces of CO observed could likely be due to by-products from remains of carbonate species left after the previous reaction/evacuation stages, which then became transformed to CO. Most likely said carbonate remains hydrogenated to formate, which in turn decomposed − slowly − into CO and H_2O, as no CO_2 production was registered.

These experimental results show that the surface of the freshly reduced catalyst is continuously modified during the onset of the RWGS reaction (and methanol synthesis), until a pseudo steady-state composition is acquired. In particular, they strongly suggest that atomic oxygen adsorbed on(to) the copper particles (R_{oxid}) is immediately produced, a fact that has certainly, and repeatedly, been reported by several workers [5,29–32].

In particular, using $Cu/ZnO/Al_2O_3$ Chinchen et al. put forward that, under methanol synthesis conditions, the coverage of oxygen (ad) sorbed on copper, O(a), is controlled by CO_2 dissociation and that the value of said coverage depends upon the p_{CO2}/p_{CO} ratio (for our Cu-Ga-Zr catalysts this aspect will be fully discussed in a forthcoming paper). Additionally, they demonstrated that this O(a) (free energy of formation, ΔG_f° = –240 kJ/mol at 513 K) is more stable than cuprous oxide, Cu_2O (ΔG_f° = –130 kJ/mol). So, they concluded that under typical alcohol synthesis conditions the state of 'operational equilibrium' of copper under steady state is Cu^0, together with a 0.3 monolayer of (ad) sorbed oxygen [30]. Meanwhile, Tang et al. demonstrated by theoretical calculations ('first principles kinetic Monte Carlo simulation') that for Cu/ZrO_2 catalysts there is 'a sinergetic effect' that allows CO_2 decomposition, resulting in the presence of up to 85% atomic O(a) at the metal-support interface [33].

The initial reaction rates of the RWGS reaction ($R_{RWGS} = R_{CO}$) for Cu/ZrO_2 and $Ga_2O_3/Cu/ZrO_2$, for the three consecutive runs conducted at atmospheric pressure (0.1 MPa and 498 K, 0.1 g cat.) employing the $H_2/CO_2/Ar$ = 66/22/12 v/v gas mixture are shown in Table 2. It is worth mentioning that the ratio of moles of reactants-to-catalyst mass in all of these atmospheric pressure experiments was lower than the one used in the medium pressure series, performed at 1.6 MPa and with 1 g cat. Consequently, the non-catalytic consumption of reactants that modifies the catalysts' surface at the earlier stages of the experiments was larger, and lasted longer, in these last low-pressure series (compare the non-linear, onset regions in Figs. 2 and 3). The rates were then calculated using the recorded values of Y_{CO} in the linear region of CO production (the 10 to 40 min time interval), as explained above.

For each catalyst, the initial rates of the RWGS reaction at medium vs. atmospheric pressure were similar (see values in Table 1 vs. Table 2), but on the binary Cu/ZrO_2 catalyst said reaction rates were somewhat higher at 1.6 MPa (approx. 40%). Also, the initial rate on this catalyst decreased by approx. 20% with the consecutive runs performed at 0.1 MPa (i.e., runs 'al', 'bl' and 'cl') whereas such trend was not observed at medium pressure. These observations might be related with

Table 2
Initial values of the reaction rate for carbon monoxide production (R_{CO}) at atmospheric pressure, for Cu/ZrO_2 and $Ga_2O_3/Cu/ZrO_2$. Experimental conditions: Gas mixtures $H_2/CO_2/Ar$ = 66/22/12 v/v and $D_2/CO_2/Ar$ = 66/22/12 v/v; T = 498 K; P = 0.1 MPa; 0.1 g cat. Consecutive runs ('*Initial*' stands for experimental data taken after the reaction onset − See text).

Catalyst	$R_{CO} \times 10^8$ (mol CO/g_{cat} .s)				
	$H_2/CO_2/Ar$ = 66/22/12			$D_2/CO_2/Ar$ = 66/22/12	
	Run[a,b]			Run[c,b]	
	'al'	'bl'	'cl'	'alD'	'blD'
Cu/ZrO_2	5.86 (0.20)[d]	4.82 (0.17)[d]	4.45 (0.15)[d]	6.32 (0.22)[d]	6.23 (0.21)[d]
	(2.65 × 10^{-3})[e]			(2.86 × 10^{-3})[e]	
$Ga_2O_3/Cu/ZrO_2$	2.12 (0.24)[d]	1.97 (0.22)[d]	1.84 (0.20)[d]	1.80 (0.20)[d]	2.07 (0.23)[d]
	(2.59 × 10^{-3})[e]			(2.20 × 10^{-3})[e]	

[a] R_{CO}: $CO_2 + H_2 \rightleftarrows CO + H_2O$ [RWGS].
[b] The values of the coefficient of determination of each linear regression for ΔY_{CO} vs. Δt within the 10 to 40 min time interval, together with the 95% confidence interval for each estimated rate value is given in Supplementary material, Table S.2.
[c] R_{CO}: $CO_2 + D_2 \rightleftarrows CO + D_2O$ [(D)RWGS].
[d] Parentheses: Surface-normalized rates, R × 10^8 (mol/m^2_{cat}.s).
[e] Turnover frequencies expressed as molecules of CO per copper surface atom per second.

the fact that, depending upon total pressure, the RWGS reaction took place simultaneously on copper and on the ZrO_2 support, as it is discussed and analyzed in more detail below. Overall, similar trends with regard to the initial rates of the RWGS reaction were observed in the gallium promoted, ternary catalyst, $Ga_2O_3/Cu/ZrO_2$.

Fig. 6 shows the Y_{CO} values that were measured conducting the RWGS using a reaction mixture containing deuterium instead of hydrogen, under the same experimental conditions as before (0.1 MPa, 498 K, $D_2/CO_2/Ar$ = 66/22/12 v/v, 0.1 g cat.) for two consecutive runs made with both catalysts, Cu/ZrO_2 and $Ga_2O_3/Cu/ZrO_2$ (labeled 'alD' and 'blD' hereafter). The time evolution of the molar fractions of the remaining component of the reaction system is given in the Supplementary material section (Figs. S.17–S.20). The experimental error of the Y_{D2O} measurement in these isotope studies was higher (~ 15%), because the most important signal for deuterated water (m/z = 20, D_2O^+) superimposed with that of Ar^{++} and because, in addition, its signal intensity (response factor) is low. A thermodynamic isotope effect ensues upon using D_2 instead of H_2 in the RWGS reaction: K_D/K_H ~ 6 (see Appendix A). Consequently, the equilibrium molar fractions of CO and D_2O are higher than in the experiments carried out with

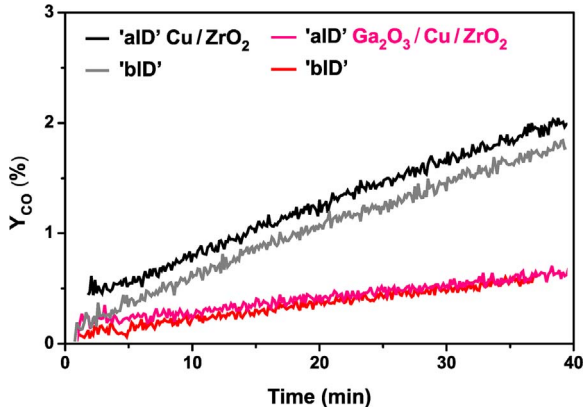

Fig. 6. CO production in the RWGS reaction at atmospheric pressure, for Cu/ZrO_2 and $Ga_2O_3/Cu/ZrO_2$, using deuterium instead of hydrogen ($D_2/CO_2/Ar$ = 66/22/12 v/v; runs 'alD' and 'blD'), at 0.1 MPa, 498 K (0.1 g cat.).

H_2/CO_2. Kunkes et al. obtained experimental values of K_D/K_H ~ 5.1 at 523 K using a ternary gas feed [7].

It can be noticed in Fig. 6 (binary catalyst) that the onset (i.e., the transient period) was shorter than in the experimental runs made with hydrogen (Fig. 3) and, also, that the molar fraction of CO during said transient was smaller. So, taking into account that CO is produced at the earlier stages of the reaction via the dissociative adsorption of CO_2 on copper, and assuming that said reaction (R_{oxid}) constitutes an intrinsic part of the catalytic cycle for the RWGS (i.e., the 'dissociative mechanism'), such decrease in the production of CO can be readily ascribed to a direct kinetic isotope effect acting on the rate of the atomic surface oxygen reduction step. This is in complete agreement with Tang et al.'s calculations, which indicate that for the RWGS on Cu/ZrO_2 the removal of the oxidative species is kinetically slow [33].

In other words, assuming that the rate determining step (*rds*) of the RWGS during the transient reaction period was the combination of surface atoms of hydrogen(deuterium) with that of oxygen (from the *facile* dissociation of CO_2 onto the surface of the completely pre-reduced metal surface at the beginning of the experiment):

$$H-\bullet + O-\bullet \rightleftarrows HO-\bullet + \bullet$$

or

$$D-\bullet + O-\bullet \rightleftarrows DO-\bullet + \bullet$$

this would lead to:

$$R_H = k_H \,.\, \theta_{O-} \,.\, \theta_{H-} \quad \text{or} \quad R_D = k_D \,.\, \theta_{O-} \,.\, \theta_{D-} \tag{1}$$

With k_H/k_D ~ 1.5 (see Appendix B) and θ_H/θ_D higher than 1 at 498 K [34–36], the 'reduction' rate of the superficial atomic oxygen would be higher with hydrogen than with deuterium (ad)atoms, which in turn would lead to a larger production of CO from the dissociative adsorption of CO_2 for the H_2/CO_2 reaction mixture instead of D_2/CO_2, during these first 10 min of reaction, as observed in Fig. 6.

On the other hand, Table 2 displays the initial rate values of the RWGS ($R_{CO} = R_{(D)RWGS}$) calculated within the 10–40 min interval (once more: after the onset period) for the two consecutive experiments carried out using D_2/CO_2, runs 'alD' and 'blD', and for the Cu/ZrO_2 and $Ga_2O_3/Cu/ZrO_2$ catalysts, at 0.1 MPa and 498 K ($D_2/CO_2/Ar$ = 66/22/12 v/v, 0.1 g cat.). The comparison of these values with the ones calculated for the conventional H_2/CO_2 gas mixture (Table 2) do not show significant differences in catalytic performance. If anything, it appears to be only a slight minor inverse kinetic isotope effect ($R_{RWGS} < R_{(D)RWGS}$) of approx. 30%, observable on the binary Cu/ZrO_2 catalyst. Nonetheless, this allows postulating, *prima facie*, that once a pseudo steady-state is reached on the catalyst surface, none of the elementary steps of the RWGS that could be considered as *rds* would involve breaking any molecular bond involving hydrogen, because if that were the case a direct kinetic isotope kinetic effect would have been observed ($k_H > k_D$) − See Appendix B −.

3.3. RWGS analysis via competing kinetic models (Model discrimination)

After obtaining the initial reaction rates of the RWGS reaction on Cu/ZrO_2 and $Ga_2O_3/Cu/ZrO_2$ from H_2/CO_2 using medium (1.6 MPa) and atmospheric pressure (0.1 MPa), as well as D_2 at 0.1 MPa, it is interesting to inquire about whether the experimental data taken after the onset of the reaction (that is, after a pseudo steady-state was already achieved) could be correlated with theoretical predictions derived from the reaction pathways reported in the literature for supported metal catalysts. In particular, it is most appealing to examine whether the metal, or the support, or both, are responsible for the observed catalytic performance.

Considering the metal surface as the sole responsible − as a first alternative − it is worth recalling that for copper-based supported catalysts several authors have postulated the dissociative mechanism as the appropriate choice [12,37,38]. On these grounds, the following

elementary reaction steps, DS_i, occurring on the metal sites (•) apply:

$$CO_2 + 2\bullet \rightleftarrows CO-\bullet + O-\bullet \quad (DS_1)$$

$$H_2 + 2\bullet \rightleftarrows 2\,H-\bullet \quad (DS_2)$$

$$H-\bullet + O-\bullet \rightleftarrows HO-\bullet + \bullet \quad (DS_3)$$

$$HO-\bullet + H-\bullet \rightleftarrows H_2O-\bullet + \bullet \quad (DS_4)$$

$$H_2O-\bullet \rightleftarrows H_2O + \bullet \quad (DS_5)$$

$$CO-\bullet \rightleftarrows CO + \bullet \quad (DS_6)$$

Using the Langmuir-Hinshelwood-Hougen-Watson (LHHW) formalism (see Appendix C), different expressions for the rate of the RWGS proceeding on said surface copper sites, but taking as rate determining step every one that does not imply the breakage of any H(D) bond, can be obtained. Table S.3 (Supplementary material section) contains the different kinetic rate expressions that were derived contemplating successively the dissociative adsorption of CO_2 (Model 1), CO desorption (Model 2), or the desorption of H_2O (Model 3) as possible *rds*.

Likewise, selecting a monofunctional, associative mechanism operating on the metal surface in which carboxyl is the key intermediate, as suggested by several authors [7,9–11,16], the following sequence of elementary reaction steps, AS_i, results:

$$H_2 + 2\bullet \rightleftarrows 2\,H-\bullet \quad (AS_1)$$

$$CO_2 + \bullet \rightleftarrows CO_2-\bullet \quad (AS_2)$$

$$CO_2-\bullet + H-\bullet \rightleftarrows HOCO-\bullet + \bullet \quad (AS_3)$$

$$HOCO-\bullet + \bullet \rightleftarrows CO-\bullet + HO-\bullet \quad (AS_4)$$

$$CO-\bullet \rightleftarrows CO + \bullet \quad (AS_5)$$

$$HO-\bullet + H-\bullet \rightleftarrows H_2O-\bullet + \bullet \quad (AS_6)$$

$$H_2O-\bullet \rightleftarrows H_2O + \bullet \quad (AS_7)$$

On the other hand, considering a bifunctional, associative mechanism on both the metal (•) and the support sites (*), and formate as the key carbonaceous intermediate [13–15], the following sequence of elementary reaction steps, AS'_i, results:

$$H_2 + 2\bullet \rightleftarrows 2\,H-\bullet \quad (AS'_1)$$

$$2 \times (H-\bullet + * \rightleftarrows H-* + \bullet) \quad (AS'_2)$$

$$CO_2 + * \rightleftarrows CO_2-* \quad (AS'_3)$$

$$CO_2-* + H-* \rightleftarrows HCOO-* + * \quad (AS'_4)$$

$$HCOO-* + * \rightleftarrows CO-* + HO-* \quad (AS'_5)$$

$$CO-* \rightleftarrows CO + * \quad (AS'_6)$$

$$HO-* + H-* \rightleftarrows H_2O-* + * \quad (AS'_7)$$

$$H_2O-* \rightleftarrows H_2O + * \quad (AS'_8)$$

Again, by means of the LHHW formalism additional kinetic rate expressions were derived considering as rate determining step (*rds*) every one that does not imply the breakage of any H(D) bond, taking CO desorption (elementary step AS_5 – Model 4 – or AS'_6 – Model 4′-), or water desorption (elementary step AS_7 – Model 5 – or AS'_8 – Model 5′-) as *rds*, because for zirconia or copper CO_2 adsorption is not judged to be rate limiting [7,12] (see Supplementary material section, Table S.3).

The inspection of the kinetic rate expressions for the RWGS reaction of Table S.3 indicates that the denominators in Models 2 to 5 include the partial pressures of CO and H_2O, which would imply, for *initial* rates (that is, whenever the approach to chemical equilibrium is still negligible), that the observed reaction rate should have been significantly dependent on said partial pressures. Because within the 10–40 min time interval this was not observed at all (the reaction rate was constant, see Fig. 3), Model 1 appears as the most adequate.

Considering now that for the reaction conditions employed in this work the most important term in the denominator of Model 1 is the one related to the coverage of the copper surface by hydrogen [40], the following simplified expression can be obtained for initial reaction conditions:

$$R_{RWGS} = R_{DS1} = \frac{k_1\ p_{CO2}\ [\bullet]^2_{Tot}}{K_2\ p_{H2}} \quad (2)$$

Because each partial pressure is related to the respective molar fraction and the total pressure of the system, P_T:

$$p_i = Y_i\ .\ P_T \quad (3)$$

the initial reaction rate, as indicated by Eq. (2), should be independent upon the total pressure. This is entirely consistent with the similar values of the measured reaction rates of the RWGS found at 0.1 and 1.6 MPa (see Tables 1 and 2).

Eq. (2) also allows analyzing the kinetic isotope effect in the experiments performed at 0.1 MPa employing the H_2/CO_2 and D_2/CO_2 stoichiometric mixtures. In said initial kinetic rate expression the only predicted difference upon using H_2 vs. D_2 is the value of the thermodynamic equilibrium constant of the elementary step corresponding to hydrogen(deuterium) dissociation, K_2. Because at 498 K said equilibrium constant exhibits a positive (thermodynamic-caused) isotope effect, ($K_{2(H)}/K_{2(D)} \sim 1.1–1.6$) [34–36] the reaction rate predicted by Eq. (2) for the D_2/CO_2 mixture should be somewhat higher, as it was experimentally found (that is, a small *inverse* kinetic isotope effect was observed). Summarizing, a dissociative pathway on the copper surface allows explaining the experimental observations of the initial reaction rate of the RWGS (which was approximately constant in the 10 to 40 min interval) on the Cu/ZrO_2 binary catalyst. In the Supplementary material section the experimental catalytic activity data shown in Fig. 3 for Cu/ZrO_2 and the calculated values obtained from the postulated equation given by Model 1 are compared, showing a fairly reasonable good fit.

Up to this point only a thermodynamic-caused isotope effect was invoked to account for the experimentally observed *initial* reaction rates (after the pseudo steady-state was achieved – 10–40 min –) but, indeed, questions might arise in regards a possible compensation between kinetic rate constants and surface coverage with the active species upon using H_2 vs. D_2. It is then appropriate to analyze the expressions for the kinetic rate constant that would have been obtained by assuming the breakage of a H(D) bond as *rds*, instead, considering both the dissociative pathway on copper and the monofunctional and bifunctional associative mechanisms.

The Supplementary material section contains detailed analyses of these alternatives (Table S4). In regards the dissociative pathway (Models 6 and 7 – Table S.4), the model expressions predict a direct kinetic isotope effect on the reaction rate, which should be lower with D_2 instead of H_2. This is at variance with the experimental findings, as shown in Table 2. On the other hand, all of the kinetic rate expressions derived by postulating that reaction steps using an associative pathway, both monofunctional (Models 8 and 9 – Table S.4) and bifunctional (Models 8′ and 9′ – Table S.4), might be rate determining, predict substantial increase of the reaction rate (above 100%) upon increasing the total pressure of the reacting system and/or using hydrogen instead of deuterium. Thus, the predictions of these models fail to adequately match the experimental data. Nonetheless, it is not unlikely that the higher RWGS reaction rates found at 1.6 vs. 0.1 MPa (approx. 40%, on average) might be indicative that associative pathways are also operating at the intermediate pressure together with the predominant, dissociative pathway on the metal, being the latter the only operative pathway at atmospheric pressure. Same conclusion (that is, CO_2 dissociation as *rds*) was found using Cu(110) – under specific conditions- [39], Cu(111) and Cu(100) – assuming a redox mechanism– [10] as

model catalysts, and for Cu/ZrO_2 [33].

The lower catalytic activity for the RWGS reaction of $Ga_2O_3/Cu/ZrO_2$ precluded us from undertaking further analyses of its initial reaction rate data. Be that as it may, no recognizable kinetic isotope effect was observed upon using D_2 instead of H_2 with this catalyst. Nonetheless, the general trends observed in regard to the RWGS rate changes with total pressure, and/or among consecutive runs, were similar for both catalysts (Tables 1 and 2). Consequently, we surmise that the predominant reaction pathway on the ternary catalyst is also dissociative, on the metal surface, as it was found for Cu/ZrO_2. Any other possible *rds* would imply non-linear increase of the molar fraction of CO (Models 2–7 −Table S.6), significant rate change with total pressure (Models 2–6 and 8,9 −Table S.6) and/or an observable kinetic isotope effect (Models 6–9 −Table S.6).

The former observations and inferences allow a more precise explanation of the selectivity improvement observed in the ternary Ga-Cu-Zr catalyst, as compared with the binary one: Because the RWGS reaction −the main responsible of selectivity decrease in methanol synthesis- occurs mainly on the copper surface (at least under usual process conditions), and taking into account that the ternary catalyst exhibited lower metal dispersion, its specific activity (that is, per catalyst mass) in the RWGS reaction was lower than that of Cu/ZrO_2, even though both catalysts showed equal metal surface-normalized reverse shift rates. Yet, the intrinsic activity of $Ga_2O_3/Cu/ZrO_2$ toward the methanol synthesis proper (R_{CH3OH}) was not affected, as the supply rate of dissociated hydrogen was still higher [19,21] and, therefore, the catalyst selectivity became improved.

Because “the exact mechanisms, the structural details, and the stability of the relevant chemistry in real catalysts remain an open question for the truly rational design of these types of synergetic catalysts” [7] we believe that the reaction engineering-based approach hereby presented, in association with the direct insight provided by spectroscopic and theoretical (DFT) analyses, can help to increase substantially the overall selectivity toward methanol from CO_2 hydrogenation.

4. Conclusions

Transient experiments on pre-reduced Cu/ZrO_2 and $Ga_2O_3/Cu/ZrO_2$ employing a Carberry-type microreactor in the batch mode and a H_2/CO_2 mixture, at 498 K, showed stoichiometric changes of the surface structure of these supported catalysts at the onset of the reaction, both at medium and atmospheric pressure (1.6 and 0.1 MPa), from the completely reduced state to one for which a build-up of atomic and molecular (ad)species set in. Said changes were revealed by continuous MS monitoring. The use of a lower ratio of moles of reactants to catalyst mass allowed concluding that adsorbed atomic oxygen on copper (but not a Cu_2O phase) was formed at said early stage.

The performance of Cu/ZrO_2 and $Ga_2O_3/Cu/ZrO_2$ in the RWGS was similar both at 1.6 and 0.1 MPa. Also, after the onset period (reaction transient during the first minutes) the initial reaction rate using the D_2/CO_2 stoichiometric mixture was slightly higher than with H_2/CO_2.

These observations were rationalized with a reaction mechanism featuring the dissociative adsorption of H_2 and CO_2 on the metal sites, and further reaction of the hydrogen moiety (H-•) and atomic oxygen (O-•) on said surface, using a simplified LHHW kinetic model. The dissociative adsorption model explains the direct kinetic isotope effect observed during the first minutes of reaction (non linear zone of CO evolution in the gas phase), where the rate determining step (*rds*) is the surface reaction between atomic oxygen and hydrogen. In addition, the dissociative adsorption of CO_2 on Cu as *rds* explains the inverse, thermodynamic-caused, isotope effect observed after the onset period and up to 40 min on stream (linear zone of CO evolution in the gas phase). The simplified model rightly predicts that the rate of the RWGS reaction is almost independent of the total pressure.

The present findings and analyses help to unveil the underlying cause(s) for the enhanced selectivity of the gallia-promoted Cu/ZrO_2 catalyst, as compared to the unpromoted one, under typical methanol synthesis conditions [18].

Acknowledgements

The financial support of UNL, CONICET (PIP 0278), and ANPCyT (PICT 0836) is gratefully acknowledged by the authors.

Appendix A. Evaluation of the thermodynamic isotope effect in the RWGS [41]

Given the reaction:$CO_2 + H_2 \leftrightarrow + H_2O + CO$ (RWGS)

the equilibrium constants for H_2 and D_2 as reactants can be expressed, in terms of the respective partition functions, as follows:

$$K_H = \frac{Q_{CO} \cdot Q_{H2O}}{Q_{H2} \cdot Q_{CO2}} \tag{A.1}$$

$$K_D = \frac{Q_{CO} \cdot Q_{D2O}}{Q_{D2} \cdot Q_{CO2}} \tag{A.2}$$

The ratio between both equilibrium constants is:

$$\frac{K_D}{K_H} = \frac{Q_{D2O}}{Q_{H2O}} \cdot \frac{Q_{H2}}{Q_{D2}} \tag{A.3}$$

Each partition function ratio can be expressed as:

$$\frac{Q_D}{Q_H} = \left[\frac{M_D}{M_H}\right] \cdot \left[\frac{(I_A I_B I_C)_D}{(I_A I_B I_C)_H}\right] \cdot \left[\prod_i^6 \frac{[1-\exp(-h\nu_{i(H)}/kT)]}{[1-\exp(-h\nu_{i(D)}/kT)]}\right] \cdot \left[\exp\left(\frac{E_{0(H)} - E_{0(D)}}{RT}\right)\right] \tag{A.4}$$

where M is molecular weight, I is inertia moment, ν_i is the ith. fundamental frequency, E_0 is zero energy, h is the Planck constant and k is the Boltzmann constant.

Because the fourth bracket in Eq. (A.4) is the most important one, the ratio between the equilibrium constants can be directly calculated as:

$$\frac{K_D}{K_H} = \exp\left(\frac{(E_{0(H2O)} - E_{0(D2O)}) + (E_{0(D2)} - E_{0(H2)})}{RT}\right) \tag{A.5}$$

From the values of each zero energy differences, equal to 1.8 kcal/mol and 3.56 kcal/mol for H_2/D_2 and H_2O/D_2O respectively, the obtained thermodynamic isotope effect at 498 K is $K_D/K_H = 5.92$.

Appendix B. Evaluation of the kinetic isotope effect in the RWGS [41]

Given the reaction:

$CO_2 + H_2 \leftrightarrow + H_2O + CO$ (RWGS)

from the absolute reaction rate theory, every reaction rate constant is proportional to the activation equilibrium constant, $K^{\#}$:

$$K^{\#} = \frac{Q^{\#}}{Q_R} \tag{A.6}$$

in which Q_R y $Q^{\#}$ are the partition functions of the adsorbed reactants and the activated state, respectively. Considering carbon dioxide as the common reactant in RWGS and (D)RWGS, then:

$$\frac{k_H}{k_D} = \frac{Q_H^{\#}}{Q_{R-H2}} \frac{Q_{R-D2}}{Q_D^{\#}} = \exp\left(\frac{(E_{0(D)}^{\#} - E_{0(H)}^{\#}) + (E_{0(H2)} - E_{0(D2)})}{RT}\right) \tag{A.7}$$

From the values of each zero energy differences for the activated states and each of the reactant considered, equal to 1.4 kcal/mol and 1.8 kcal/mol, respectively, $k_H/k_D = 1.5$ at 498 K.

Appendix C. Competitive models for the evaluation of the reaction rate of the RWGS using the Langmuir-Hinshelwood-Hougen-Watson (LHHW) formalism

(A.8) Dissociative mechanism, on the metal sites (•):

$CO_2 + 2\bullet \leftrightarrow CO-\bullet + O-\bullet$ (DS_1)

$H_2 + 2\bullet \leftrightarrow 2H-\bullet$ (DS_2)

$H-\bullet + O-\bullet \leftrightarrow HO-\bullet + \bullet$ (DS_3)

$HO-\bullet + H-\bullet \leftrightarrow H_2O-\bullet + \bullet$ (DS_4)

$H_2O-\bullet \leftrightarrow H_2O + \bullet$ (DS_5)

$CO-\bullet \rightleftarrows CO + \bullet$ (DS_6)

Model 1 (as an example): Dissociative adsorption of CO_2 (DS_1) as rate determining step (*rds*) and the following reaction steps in thermodynamic equilibrium:

$$K_2 = \frac{[H-\bullet]^2}{p_{H2}\ [\bullet]^2} \tag{A.8}$$

$$K_3 = \frac{[HO-\bullet]\ [\bullet]}{[H-\bullet]\ [O-\bullet]} \tag{A.9}$$

$$K_4 = \frac{[H_2O-\bullet]\ [\bullet]}{[HO-\bullet]\ [H-\bullet]} \tag{A.10}$$

$$K_5 = \frac{p_{H2O}\ [\bullet]}{[H_2O-\bullet]} \tag{A.11}$$

$$K_6 = \frac{p_{CO}\ [\bullet]}{[CO-\bullet]} \tag{A.12}$$

Where K_i: equilibrium constant of the ith reaction, p_j: partial pressure of the jth reactant/product, and [X]: surface concentration of species X (X: $H-\bullet$, $O-\bullet$, $H-\bullet$, $CO-\bullet$, $HO-\bullet$, and $H_2O-\bullet$).

The balance of the total metal sites is then equal to:

$$[\bullet]_{Tot} = [\bullet] + [O-\bullet] + [CO-\bullet] + [H-\bullet] + [HO-\bullet] + [H_2O-\bullet] \tag{A.13}$$

$$[\bullet]_{Tot} = [\bullet] + \frac{1}{K_2\ K_3\ K_4\ K_5}\ \frac{p_{H2O}}{p_{H2}}\ [\bullet] + \frac{p_{CO}}{K_6}\ [\bullet] + K_2^{0.5}\ p_{H2}^{0.5}\ [\bullet] + \frac{1}{K_2^{0.5}\ K_4\ K_5}\ \frac{p_{H2O}}{p_{H2}^{0.5}}\ [\bullet] + \frac{p_{H2O}}{K_5}\ [\bullet] \tag{A.14}$$

For the elementary reaction DS_1 (step 1) as *rds* of the RWGS reaction, then:

$$R_{RWGS} = R_{DS1} = k_1\ p_{CO2}\ [\bullet]^2 - k_{-1}\ [CO-\bullet]\ [O-\bullet] \tag{A.15}$$

$$R_{RWGS} = R_{DS1} = \frac{k_1\ p_{CO2}\ [\bullet]_{Tot}^2 \left(1 - \frac{p_{CO}\ p_{H2O}}{p_{CO2}\ p_{H2}\ K_{RWGS}}\right)}{\left(1 + \frac{1}{K_2\ K_3\ K_4\ K_5}\ \frac{p_{H2O}}{p_{H2}} + \frac{p_{CO}}{K_6} + K_2^{0.5}\ p_{H2}^{0.5} + \frac{1}{K_2^{0.5}\ K_4\ K_5}\ \frac{p_{H2O}}{p_{H2}^{0.5}} + \frac{p_{H2O}}{K_5}\right)^2} \tag{A.16}$$

Appendix D. Supplementary data

Supplementary data associated with this article can be found, in the online version, at http://dx.doi.org/10.1016/j.jcou.2017.06.002.

References

[1] C.V. Ovesen, P. Stoltze, J.K. Norskov, C.T. Campbell, A kinetic model of the water gas shift reaction, J. Catal. 134 (1992) 445–468.
[2] M.S. Spencer, On the activation energies of the forward and reverse water-gas shift reaction, Catal. Lett. 32 (1995) 9–13.
[3] G. Wang, L. Jiang, Y. Zhou, Z. Cai, Y. Pan, X. Zhao, Y. Li, Y. Sun, B. Zhong, X. Pang, W. Huang, K. Xie, Investigation of the kinetic properties for the forward and reverse WGS reaction by energetic analysis, J. Mol. Struct. (Theochem.) 634 (2003) 23–30.
[4] C.T. Campbell, Micro- and macro-kinetics: their relationship in heterogeneous catalysis, Top. Catal. 1 (1994) 353–366.
[5] S. Bailey, G.F. Froment, J.W. Snoeck, K.C. Waugh, A DRIFT study of the morphology and surface adsorbate composition of an operating methanol synthesis catalyst, Catal. Lett. 30 (1995) 99–111.
[6] G.C. Chinchen, M.S. Spencer, A comparison of the water-gas shift reaction on chromia-promoted magnetite and on supported copper catalysts, J. Catal. 112 (1988) 325–327.
[7] E.L. Kunkes, F. Studt, F. Abild-Pedersen, R. Schlögl, M. Behrens, Hydrogenation of CO_2 to methanol and CO on $Cu/ZnO/Al_2O_3$: is there a common intermediate or not? J. Catal. 328 (2015) 43–48.
[8] J.F. Edwards, G.L. Schrader, Infrared spectroscopy of Cu/ZnO catalysts for the water-gas shift reaction and methanol synthesis, J. Phys. Chem. 88 (1984) 5620–5624.
[9] Y. Yang, C.A. Mims, D.H. Mei, C.H.F. Peden, C.T. Campbell, Mechanistic studies of methanol synthesis over Cu from $CO/CO_2/H_2/H_2O$ mixtures: the source of C in methanol and the role of water, J. Catal. 298 (2013) 10–17.
[10] G.C. Wang, J. Nakamura, Structure sensitivity for forward and reverse water-gas shift reactions on copper surfaces: a DFT study, J. Phys. Chem. Lett. 1 (2010) 3053–3057.
[11] L.C. Grabow, M. Mavrikakis, Mechanism of methanol synthesis on Cu through CO_2 and CO hydrogenation, ACS Catal. 1 (2011) 365–384.
[12] I.A. Fisher, A.T. Bell, In-situ infrared study of methanol synthesis from H_2/CO_2 over Cu/SiO_2 and $Cu/ZrO_2/SiO_2$, J. Catal. 172 (1997) 222–237.
[13] A. Baiker, M. Kilo, M. Maciejewski, S. Menzi, A. Wokaun, Hydrogenation of CO_2 over copper, silver and gold/zirconia, catalysts: comparative study of catalyst properties and reaction pathways, Proc.10th Int Congr. Catalysis, Budapest, Hungary, 1992, pp. 19–24.
[14] J. Wambach, A. Baiker, A. Wokaun, CO_2 hydrogenation over metal/zirconia catalysts, Phys. Chem. Chem. Phys. 1 (1999) 5071–5080.
[15] B.A. Peppley, J.C. Amphlett, L.M. Kearns, R.F. Mann, Methanol-steam reforming on $Cu/ZnO/Al_2O_3$ catalysts. Part 2. A comprehensive kinetic model, Appl. Catal. A: Gen. 179 (1999) 31–49.
[16] H. Prats, L. Álvarez, F. Illas, R. Sayós, Kinetic Monte-Carlo simulations of the water gas shift reaction on Cu(111) from density functional theory based calculations, J. Catal. 333 (2016) 217–226.
[17] L. Yang, A. Karim, J. Muckerman, Density functional kinetic Monte Carlo simulation of water-gas shift reaction of Cu/ZnO, J. Phys. Chem. C 117 (2013) 3414–3425.
[18] E.L. Fornero, P.B. Sanguineti, D.L. Chiavassa, A.L. Bonivardi, M.A. Baltanás, Performance of ternary $Cu–Ga_2O_3–ZrO_2$ catalysts in the synthesis of methanol using CO_2-rich gas mixtures, Catal. Today 213 (2013) 163–170.
[19] E.L. Fornero, A.L. Bonivardi, M.A. Baltanás, Isotopic study of the rates of hydrogen provision vs. methanol synthesis from CO_2 over Cu-Ga-Zr catalysts, J. Catal. 330 (2015) 302–310.
[20] G.C. Chinchen, C.M. Hay, H.D. Vandervell, K.C. Waugh, The measurement of copper surface areas by reactive frontal chromatography, J. Catal. 103 (1987) 79–86.
[21] P.B. Sanguineti, M.A. Baltanás, A.L. Bonivardi, Copper–gallia interaction in $Cu–Ga_2O_3–ZrO_2$ catalysts for methanol production from carbon oxide(s) hydrogenation, Appl. Catal. A: Gen. 504 (215) (2017) 476–481.
[22] E.L. Fornero, J.L. Giombi, D.L. Chiavassa, A.L. Bonivardi, M.A. Baltanás, A versatile Carberry-type microcatalytic reactor for transient and/or continuous flow operation at atmospheric or medium pressure, Chem. Eng. J. 264 (2015) 664–671.
[23] K.D. Jung, A.T. Bell, Role of hydrogen spillover in methanol synthesis over Cu/ZrO_2, J. Catal. 193 (2000) 207–223.
[24] I.A. Fisher, A.T. Bell, In situ infrared study of methanol synthesis from H_2/CO over Cu/SiO_2 and $Cu/ZrO_2/SiO_2$, J. Catal. 178 (1998) 153–173.
[25] T.C. Schilke, I.A. Fisher, A.T. Bell, In situ infrared study of methanol synthesis from CO_2/H_2 on titania and zirconia promoted Cu/SiO_2, J. Catal. 184 (1999) 144–156.
[26] G.H. Graaf, E.J. Stamhuis, A.A.C.M. Beenackers, Kinetics of low-pressure methanol synthesis, Chem. Eng. Sci. 43 (1988) 3185–3195.
[27] J. Skrzypek, M. Lachowska, H. Moroz, Kinetics of methanol synthesis over commercial copper/zinc oxide/alumina catalysts, Chem. Eng. Sci. 46 (1991) 2809–2813.
[28] K.M. Vanden Bussche, G.F. Froment, A steady-state kinetic model for methanol synthesis and the water gas shift reaction on a commercial $Cu/ZnO/Al_2O_3$ catalyst, J. Catal. 161 (1996) 1–10.
[29] S.D. Jackson, B.J. Brandreth, Non-steady-state and transient isotope tracer studies in methanol synthesis, J. Chem. Soc. Faraday Trans. 1 (85) (1989) 3579–3585.
[30] G.C. Chinchen, M.S. Spencer, K.C. Waugh, D.A. Whan, Promotion of methanol synthesis and the water-gas shift reaction by adsorbed oxygen on supported copper catalysts, J. Chem. Soc. Faraday Trans. 1 (83) (1987) 2193–2212.
[31] M. Muhler, W. Törnqvist, L.P. Nielsen, B.S. Clausen, H. Topsoe, On the role of adsorbed atomic oxygen and CO_2 in copper based metanol synthesis catalysts, Catal. Lett. 25 (1994) 1–10.
[32] L.Z. Gao, J.T. Li, C.T. Au, Mechanistic studies of CO and CO_2 hydrogenation to methanol over a 50Cu/45Zn/5Al catalyst by in-situ FT-IR, chemical trapping and isotope labeling methods, Stud. Surf. Sci. Catal. 130 (2000) 3711–3716.
[33] Q.L. Tang, Q.J. Hong, Z.P. Liu, CO_2 fixation into methanol at Cu/ZrO_2 interface from first principles kinetic Monte Carlo, J. Catal. 263 (2009) 114–122.
[34] D.K. Kim, E. Iglesia, Isotopic and kinetic assessment of the mechanism of CH_3OH-H_2O catalysis on supported copper clusters, J. Phys. Chem. C 112 (2008) 17235–17243.
[35] C.S. Kellner, A.T. Bell, Synthesis of oxygenated products from carbon monoxide and hydrogen over silica- and alumina-supported ruthenium catalysts, J. Catal. 71 (1981) 288–295.
[36] M. Kiyomiya, N. Momma, I. Yasumori, The kinetics and mechanism of hydrogen adsorption and hydrogen-deuterium equilibration on the copper surface, Bull. Chem. Soc. Japan 47 (8) (1974) 1852–1857.
[37] A.A. Gokhale, J.A. Dumesic, M. Mavrikakis, On the mechanism of low-temperature water gas shift reaction on copper, J. Am. Chem. Soc. 130 (2008) 1402–1414.
[38] Y. Yang, C.A. Mims, R.S. Disselkamp, C.H.F. Peden, C.T. Campbell, Simultaneous MS-IR studies of surface formate reactivity under methanol synthesis conditions on Cu/SiO_2, Top. Catal. 52 (2009) 1440–1447.
[39] J. Yoshihara, C.T. Campbell, Methanol synthesis and reverse water-gas shift kinetics over Cu(110) model catalysts: structural sensitivity, J. Catal. 161 (1996) 776–782.
[40] T.S. Askgaard, J.K. Norskov, C.V. Ovesen, P. Stoltze, A kinetic model of methanol synthesis, J. Catal. 156 (1995) 229–242.
[41] A. Ozaki, Isotopic Studies of Heterogeneous Catalysis, Academic Press, New York, 1977.